Copernicus FICE 2024

Training on
In situ Ocean Colour Above-Water Radiometry towards Satellite Validation

AERONET-OC

Giuseppe Zibordi

giuseppe.zibordi@eoscience.eu

PROGRAMME OF THE EUROPEAN UNION
Copernicus Europe's eyes on Earth
IMPLEMENTED BY EUMETSAT
FRM4SOC Phase-2
fiducial reference measurements for satellite ocean colour
CNR ISMAR ISTITUTO DI SCIENZE MARINE

6-17 May 2024
Venice, Italy

AERONET-OC

The outcome of an excellent NASA-JRC collaboration.

The Ocean Color component of AERONET is an asset for the major Space Agencies managing ocean color missions (e.g., EUMETSAT, KARI, NOAA, JAXA, ESA, CNSA, NASA, …) and by the ocean colour community at large.

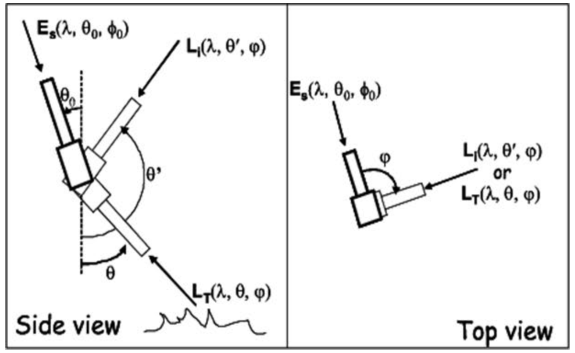

$(\varphi = \varphi_0 + 90^0; \theta = 40^0; \theta' = 140^0)$

Sky-radiance: L_i

Sea-radiance: L_T

$$L_W(\varphi,\theta,\lambda) = L_T(\varphi,\theta,\lambda) - \rho(\varphi,\theta,\theta_0,W)L_i(\varphi,\theta',\lambda)$$

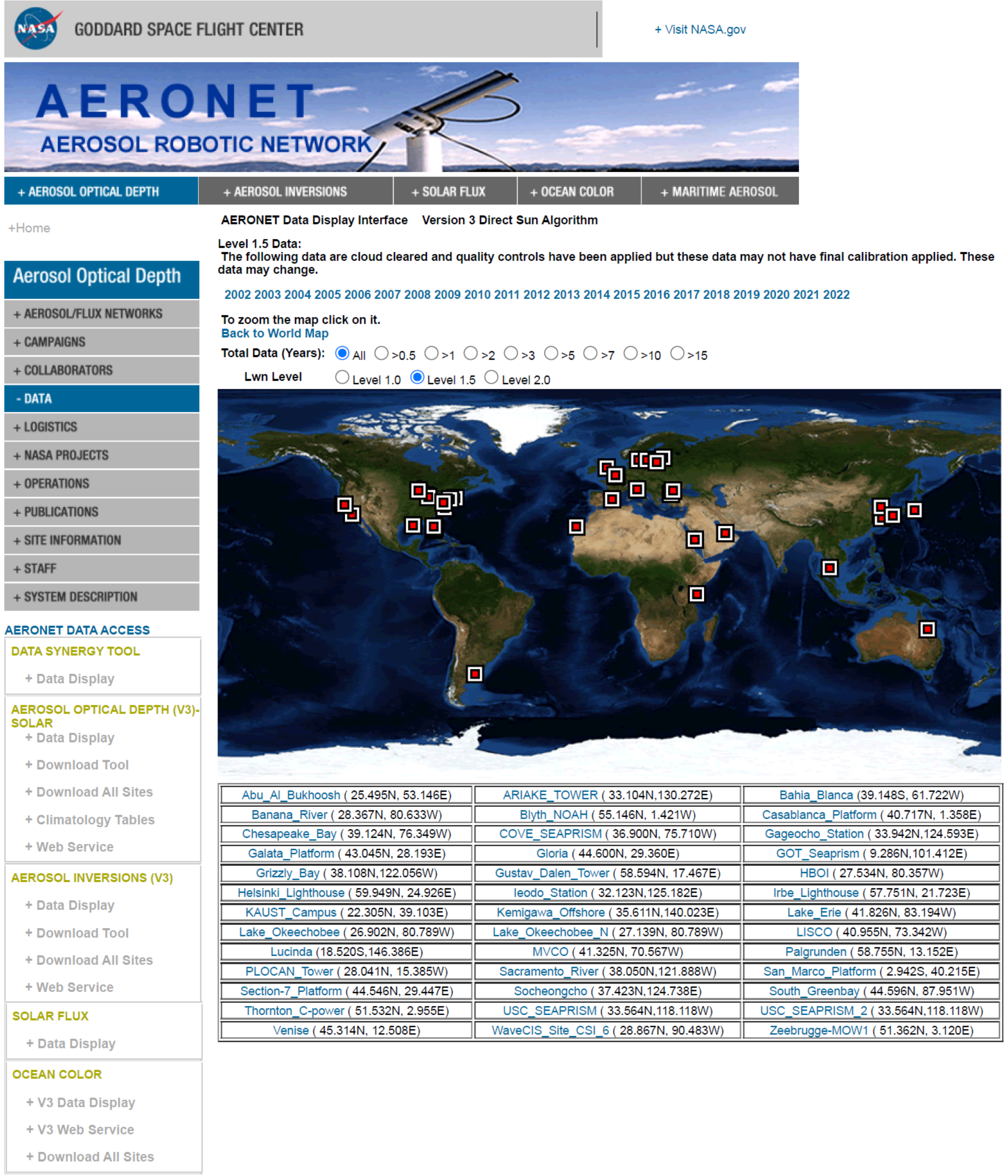

AERONET-OC: sites

The Ocean Color component of the Aerosol Robotic Network generating globally distributed time-series of standardized $L_{WN}(\lambda)$ and $\tau_a(\lambda)$ measurements targeting the validation of satellite ocean color data products

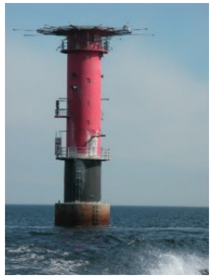

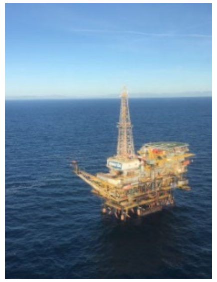

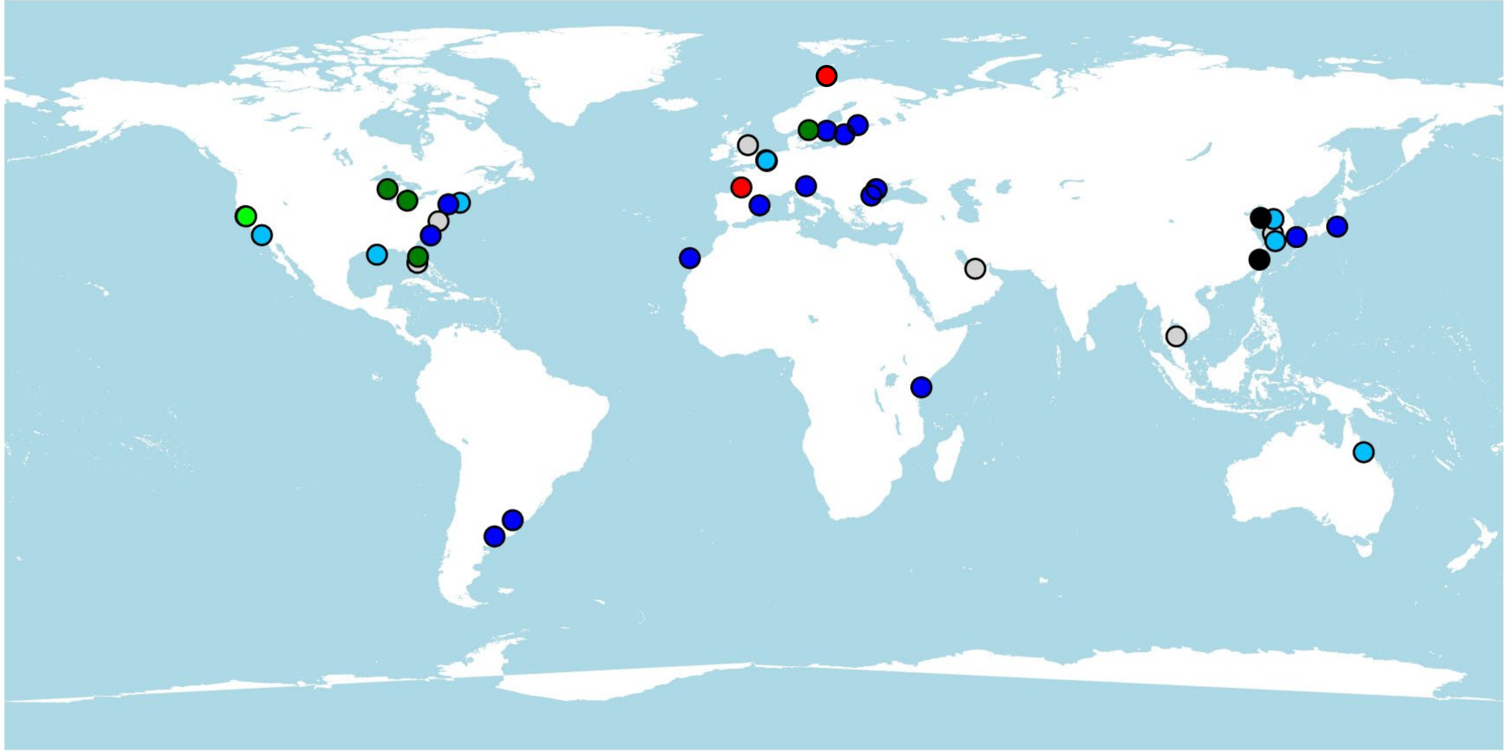

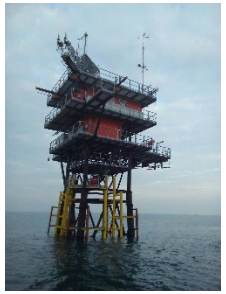

CE-318 (9-channel)

CE-318T (12-channel)

Active marine Active inland Potential Dismissed

➢ ***Active Marine sites (26,** 3 are on hold; plus 2 AERONET-OC equivalent sites managed by China whose data are not yet accessible)*

AAOT (*replacing Venice*); Ariake_Tower; Bahia_Blanca; Casablanca_Platform; Chesapeake_Bay; Frying_Pan_Platform; Galata_Platform; Gustaf_Dalen_Tower; Helsinki_LightHouse (*on hold*); Irbe_Lighthouse; Kemigawa_Offshore; LISCO; Lucinda; MVCO; PLOCAN_Tower; RdP-EsNM; San_Marco_Platform; Section-7_Platform (*replacing Gloria*); Ieodo Station (*on hold*); Socheongcho; Thornton_C-power (*on hold*); USC_SEAPRISM; WaveCIS_Site_CSI_6; Zeebrugge-MOW1; Muping; Dongou.

➢ ***Active inland sites (5)***

Palgrunden; Banana_River; Lake_Erie; South_Greenbay; Sacramento_River.

Potential sites (2)

Gulf_of_Biscay, Norwegian Sea

AERONET-OC: band settings

Multi-spectral radiometry, but benefitting of multi-decadal advancement in (fore)optics design, measurement methods, instruments handling, data management and processing.

- *CE-318 9-channel for **marine** applications (considered obsolete).*
- *CE-318T 12-channel with two standard configurations for **marine and lake** applications.*

Band settings

Satellite Sensors	Wavelengths [nm]																			
MODIS		412.5	443	488		531	551		667	678		748				870		905	940	
VIIRS (20 nm)		412	445	488			555		672			746			865					
OLCI (10 nm)	400	412.5	442.5	490	510		560	620	665	681	709	754	...	779	865		885	900	940	1020

AERONET-OC	Wavelengths [nm]																			
PRS-09		412	443	488		531	551		667							870			940	1020
PRS-12 (sea)	400	412.5	442.5	490	510		560	620	665					779	865				940	1020
PRS-12 (lake)		412.5	442.5	490	510		560	620	667	681	709				865				940	1020

AERONET-OC: sites (2002-2020)

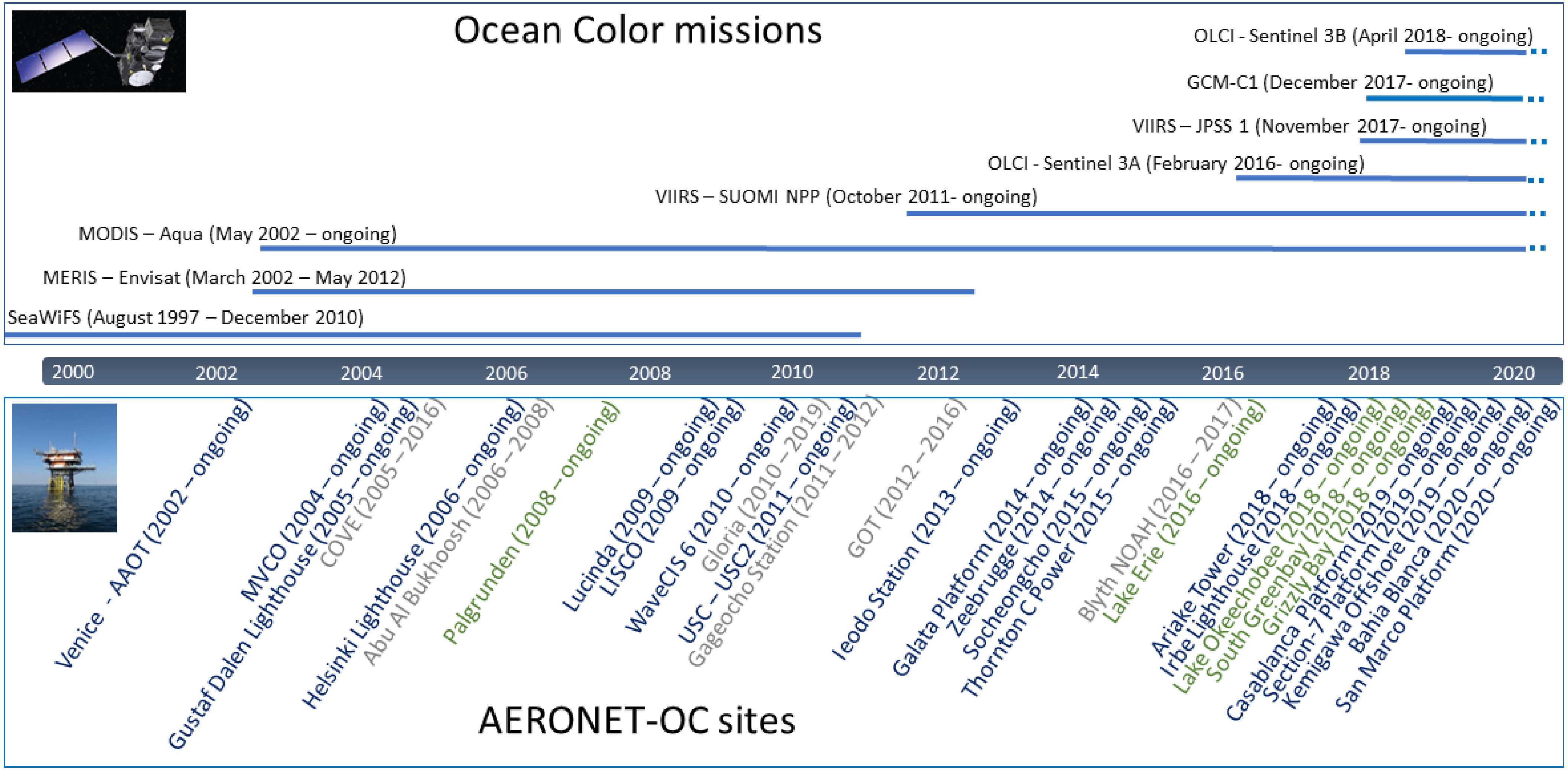

Zibordi, G., Holben, B. N., Talone, M., D'Alimonte, D., Slutsker, I., Giles, D. M., & Sorokin, M. G. (2021). Advances in the Ocean Color component of the Aerosol Robotic Network (AERONET-OC). Journal of Atmospheric and Oceanic Technology, 38(4), 725-746.

AERONET-OC: Quality Levels

AERONET-OC products are classified at different QC levels:

Level 1.0-> ▪ $L_{WN}(\lambda)$ *determined from complete measurement sequences.*

Level 1.5-> ▪ *Cloud screened aerosol optical thickness data exist;*
▪ *Replicate sky and sea radiance measurements exhibit low variance;*
▪ *Empirical thresholds are satisfied (e.g., exceedingly negative or positive values).*

Level 2.0-> ▪ *Pre- and post-deployment calibration coefficients exhibit justifiable differences within 5%;*
▪ *An automated screening is passed to determine the:*
  i. *consistency of* $L_{WN}(\lambda)$ *spectral shapes within the data set itself (spectral-consistency),*
  ii. *absence of short-term glitches or systematic daily trends (temporal consistency).*

Zibordi, G., Holben, B. N., Talone, M., D'Alimonte, D., Slutsker, I., Giles, D. M., & Sorokin, M. G. (2021). Advances in the Ocean Color component of the Aerosol Robotic Network (AERONET-OC). Journal of Atmospheric and Oceanic Technology, 38(4), 725-746.

Expert Based QC

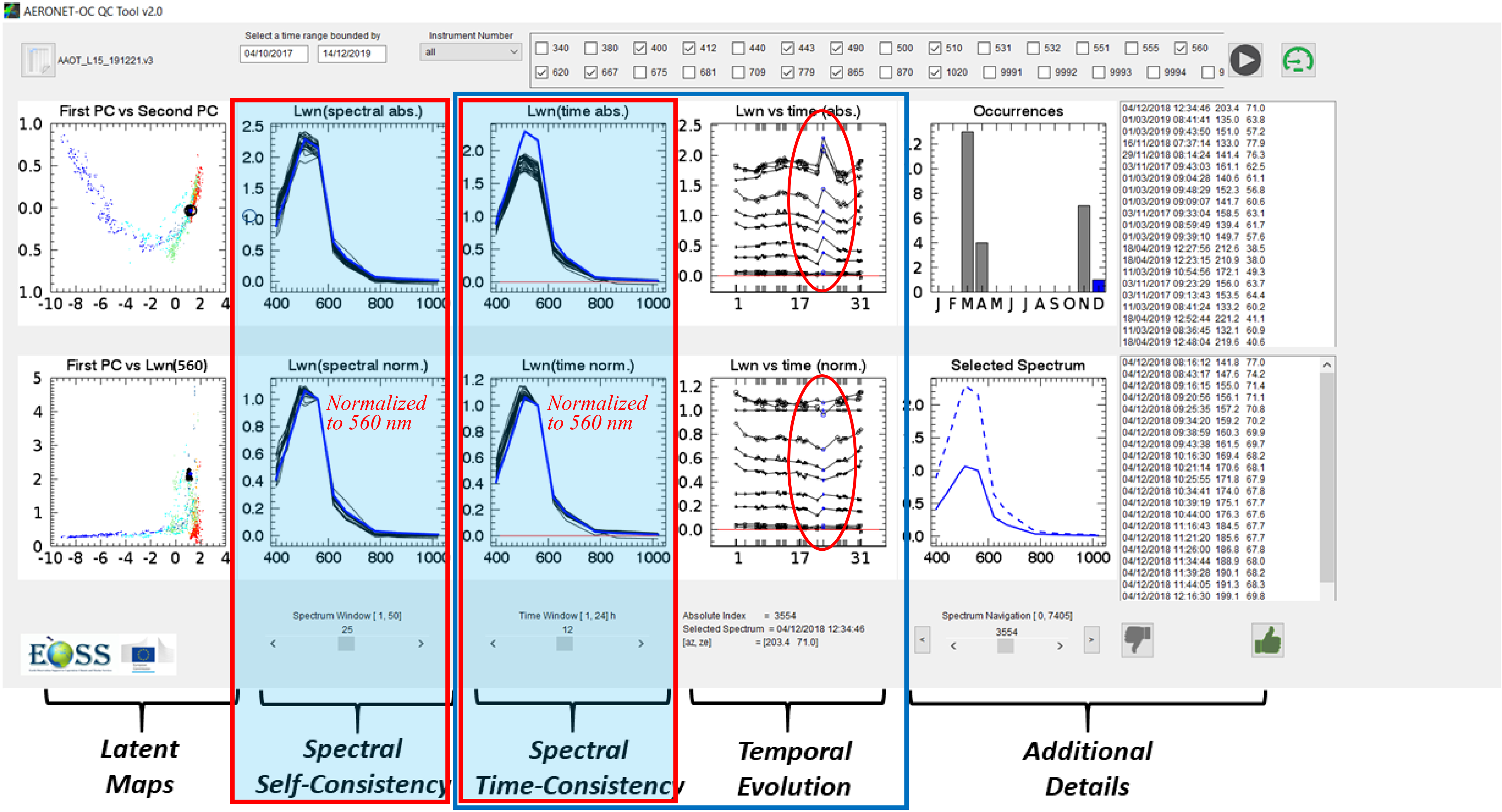

The same principles are now applied in a fully automated QC procedure

Zibordi, G., Holben, B. N., Talone, M., D'Alimonte, D., Slutsker, I., Giles, D. M., & Sorokin, M. G. (2021). Advances in the Ocean Clor component of the Aerosol Robotic Network (AERONET-OC). Journal of Atmospheric and Oceanic Technology, 38(4), 725-746.

AERONET-OC Version 4

Version-3 (https://aeronet.gsfc.nasa.gov/cgi-bin/draw_map_display_seaprism_v3)

- *Relaying on spectrally independent ρ-factors from Mobley (1999)*
- *Comprehensive and fully automated QC at Level 2.0.*
- *Data products (i.e., L_{WN}) corrected for brdf according to the Chla- and IOP-based methods.*

Toward Version-4

- *Comprehensive and fully automated QC also at Level 1.5 (i.e., incorporating most of the current quality checks applied for Level 2.0).*
- *Ranking of individual L_{WN} as a function of spectral and temporal consistency for a better assessment of satellite data products.*
- *Statistical determination of L_{WN} uncertainties for individual measurements.*
- *Application of advanced sea surface reflectance factors accounting for spectral dependence as a function of aerosol type and optical thickness, and polarization (under evaluation since April 2024).*

Zibordi, G., Holben, B. N., Talone, M., D'Alimonte, D., Slutsker, I., Giles, D. M., & Sorokin, M. G. (2021). Advances in the Ocean Color component of the Aerosol Robotic Network (AERONET-OC). Journal of Atmospheric and Oceanic Technology, 38(4), 725-746.

Early AERONET-OC data application

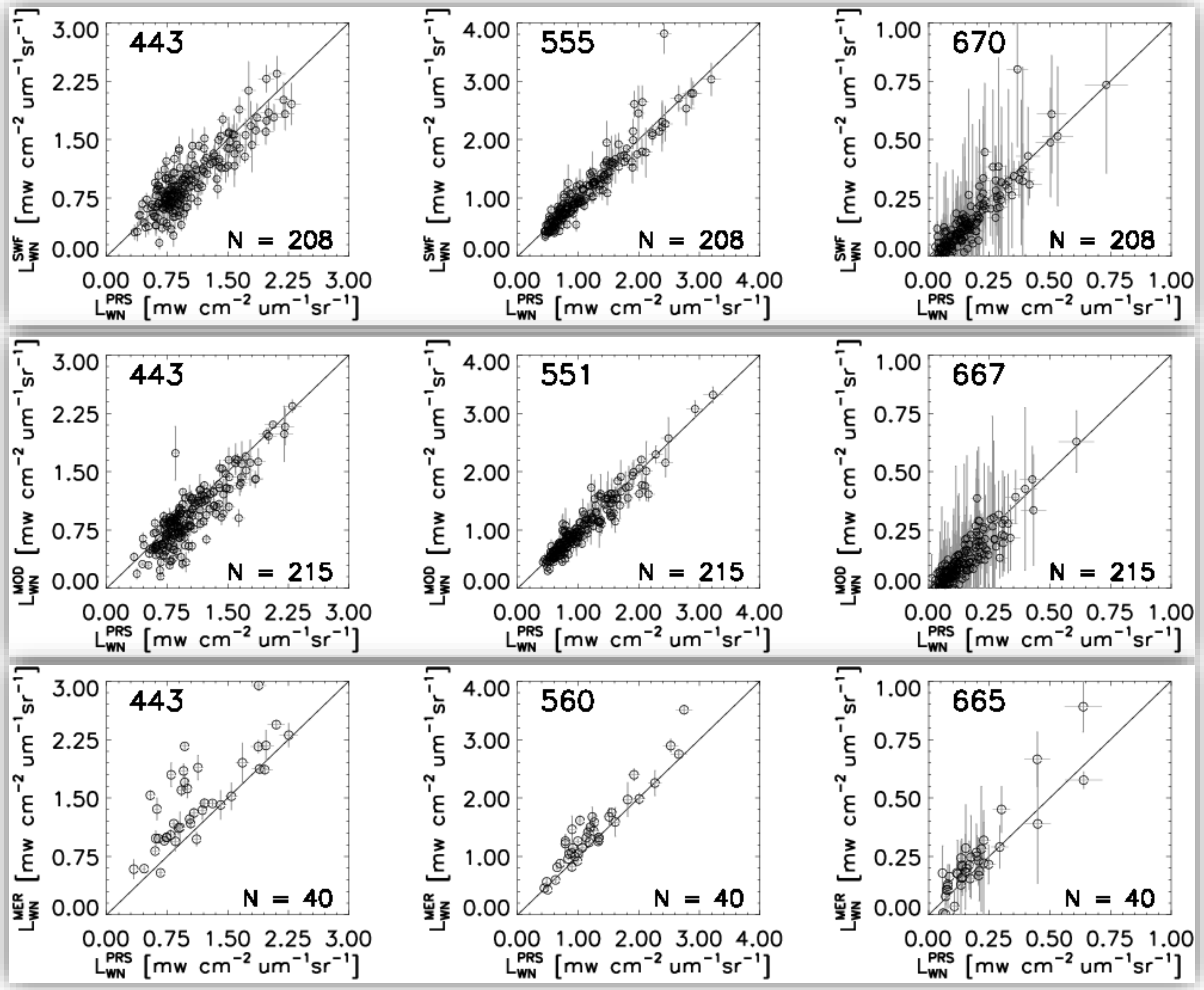

SeaWiFS vs AERONET-OC

MODIS-A vs AERONET-OC

MERIS vs AERONET-OC

These scatter plots were included in the first publication showing the relevance of autonomous above-water radiometry in support of satellite ocean colour validation activities (someone wrote that this changed the way to perform validation activities).

Zibordi, G., Mélin, F., & Berthon, J. F. (2006). Comparison of SeaWiFS, MODIS and MERIS radiometric products at a coastal site. Geophysical Research Letters, 33(6).

AERONET-OC: an automated network of above-water multi-spectral radiometers

Outline

- The network
  - Objectives
  - Sites
- Data products and access
- Applications

Copernicus FICE 2024

Training on
In situ Ocean Colour Above-Water Radiometry towards Satellite Validation

A view on the Sky-Blocked Approach

Giuseppe Zibordi

giuseppe.zibordi@eoscience.eu

PROGRAMME OF THE EUROPEAN UNION
Copernicus Europe's eyes on Earth
IMPLEMENTED BY EUMETSAT
FRM4SOC Phase-2
fiducial reference measurements for satellite ocean colour
CNR ISMAR ISTITUTO DI SCIENZE MARINE

6-17 May 2024
Venice, Italy

Near-surface radiometry

Historical dates

1990s: First successful measurements
2010s: Method assessment
2020s: Comprehensive uncertainty analysis

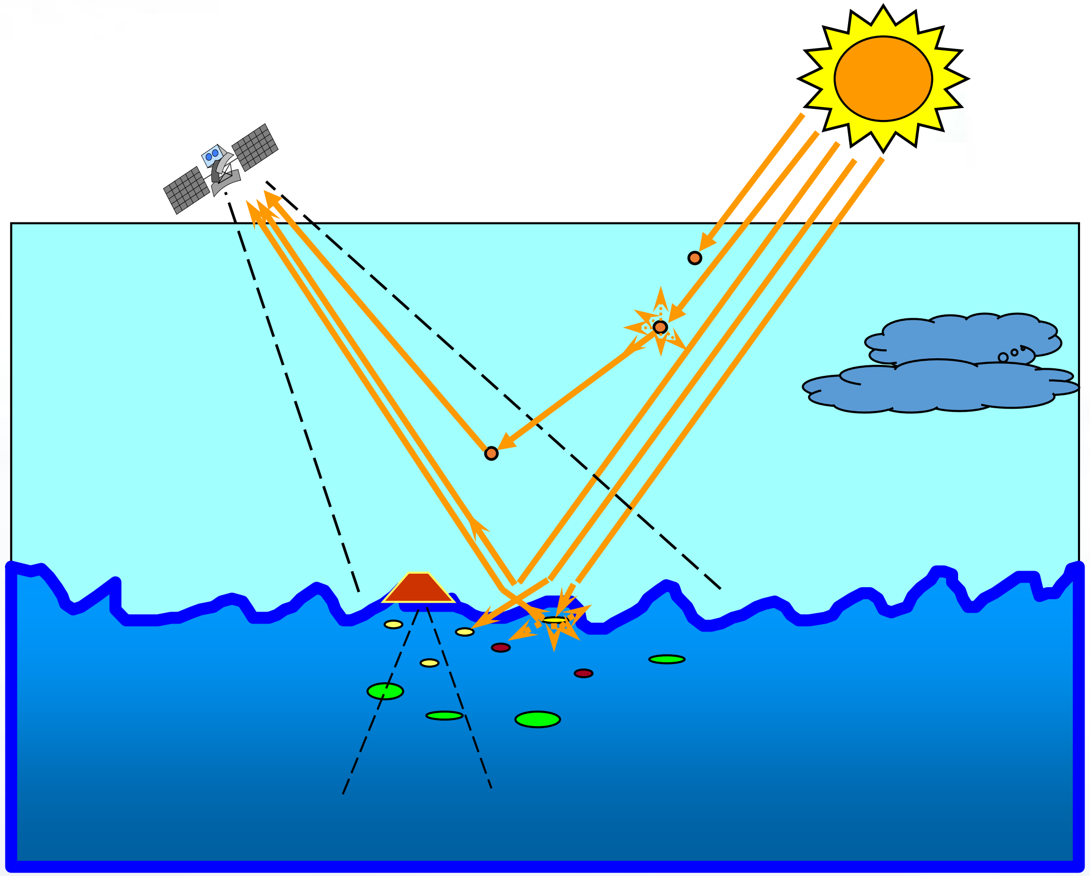

Advantages

1. Simple deployment procedure
2. Insensitive to coastal water optical stratifications

Drawback

1. Cannot produce profiles of radiometric quantities
2. Restricted to a few radiometric quantities (i.e., L_w)
3. Highly sensitive to wave perturbations
4. Requires corrections for shading perturbations and for near-surface in-water transmittance

Near-surface radiometry

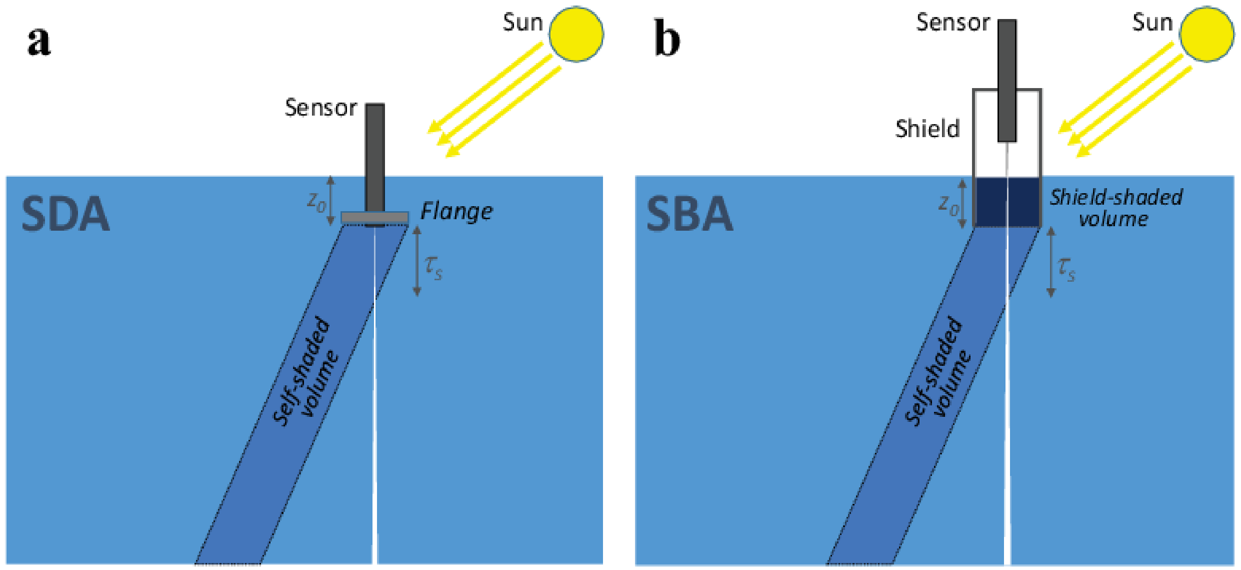

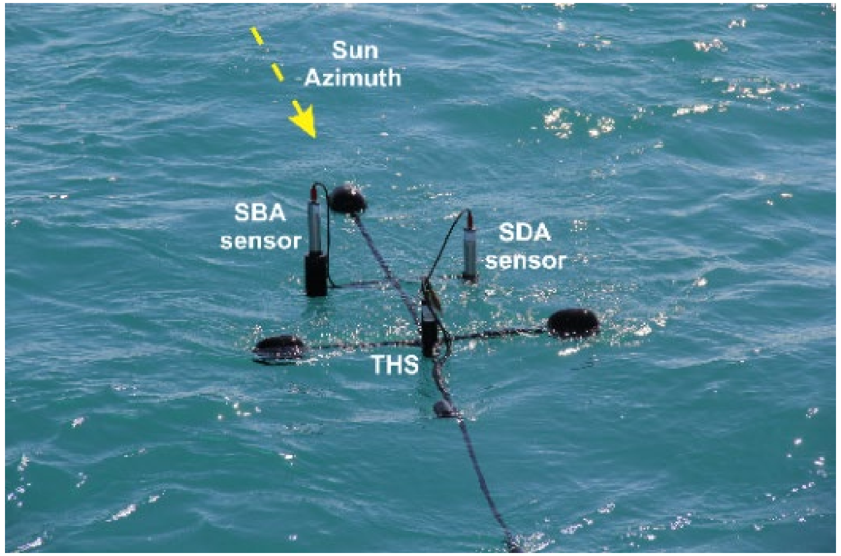

In water !

$$L_W^{SDA}(\lambda) = L_u(z_0,\lambda) \cdot C_{ss}^{SDA}(\lambda, a, I_r, \theta_0, R_d, f^{SDA}) \cdot C_{K_L}(\lambda, K_L, z_0) \cdot \frac{t_{wa}(\lambda)}{n_w^2(\lambda)}$$

Above water !

$$L_W^{SBA}(\lambda) = L_W(z_0,\lambda) \cdot C_{ss}^{SBA}(\lambda, a, I_r, R_d, f^{SBA}) \cdot C_{K_L}(\lambda, K_L, z_0) \cdot C_{is}(\lambda, a, b_b, z_0)$$

Korea Ocean Research & Development Institute (KORDI), "Development of red-tide and water turbidity algorithms using ocean color satellite," BSPE 98721-00-1224-01, (1999).

A. Tanaka, H. Sasaki and J. Ishizaka, "Alternative measuring method for water-leaving radiance using a radiance sensor with a domed cover," Opt. Express 14(8), 3099–3105 (2006).

Z. Lee, Y. H. Ahn, C. Mobley and R. Arnone, "Removal of surface-reflected light for the measurement of remote-sensing reflectance from …," Opt. Express, 18 (25), 26313–26324 (2010).

G. Zibordi and M. Talone, M. , "On the equivalence of near-surface methods to determine the water-leaving radiance." Opt. Express, 28(3), 3200-3214 (2020).

On the equivalence of near-surface radiometry

SBA was suggested to be superior to other in-water or above-water methods because of its immediacy and the capability of 'directly' measure the water-leaving radiance. For instance, SDA requires correction for the transmittance of *Lu* from below to above water in view of determining *Lw*.

SBA and SDA methods were comprehensively compared through a specific experiment requiring the design of a dedicated measuring system and the collection of data in a number of diverse water types.

Research Article Vol. 28, No. 3 / 3 February 2020 / *Optics Express* 3200

Optics EXPRESS

On the equivalence of near-surface methods to determine the water-leaving radiance

GIUSEPPE ZIBORDI* AND MARCO TALONE

Joint Research Centre of the European Commission, Ispra, Italy

**giuseppe.zibordi@ec.europa.eu*

Errors quantification

Corrections for the non linear response

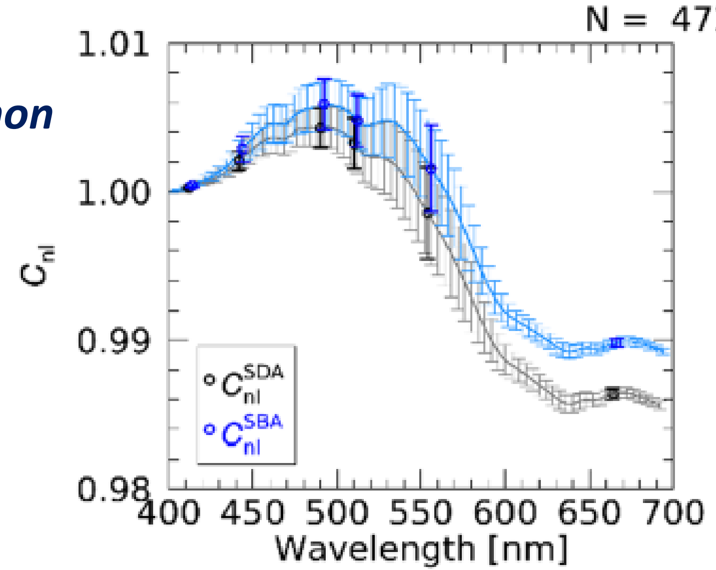

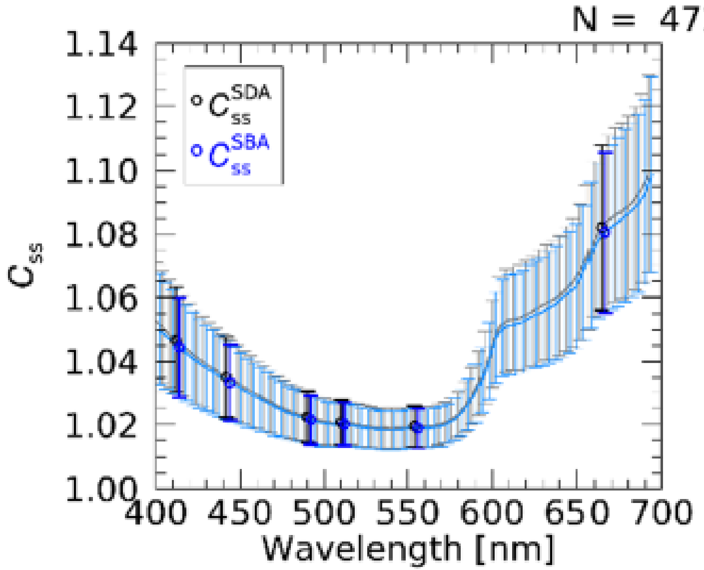

Corrections for self-shading perturbations

Correction for the water attenuation between the depths z_0 and 0^-

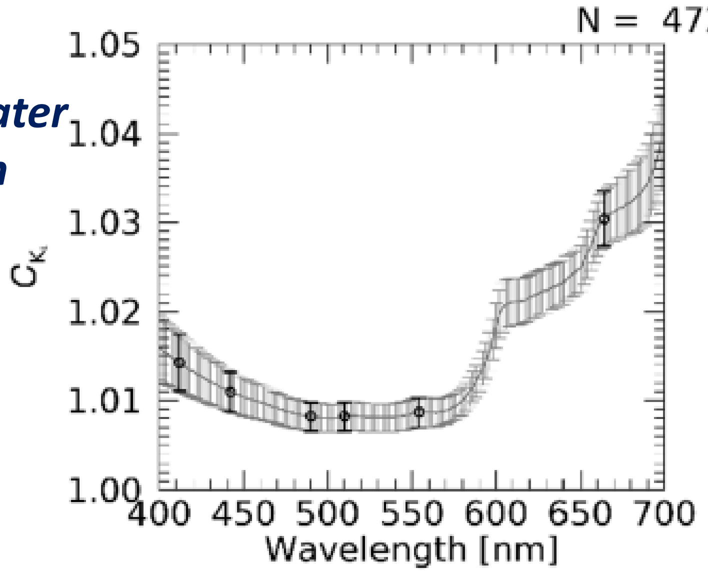

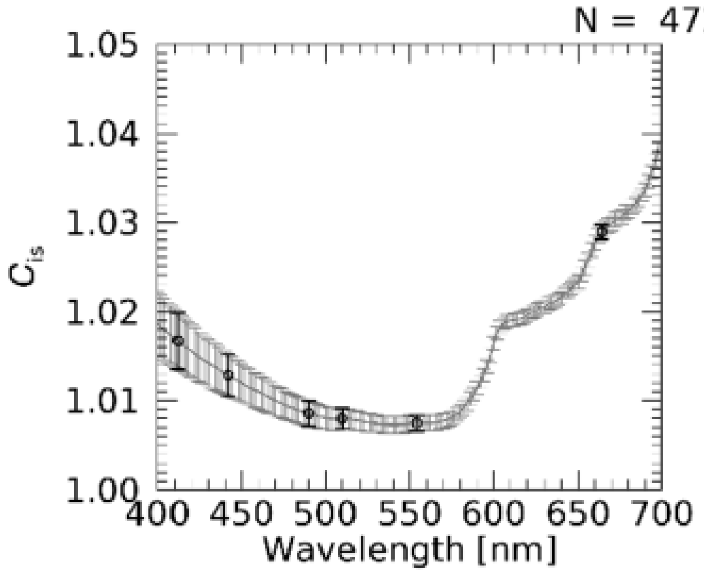

Corrections for the immersed portion of the shield

… and what about the water likely splashing on the optical window?

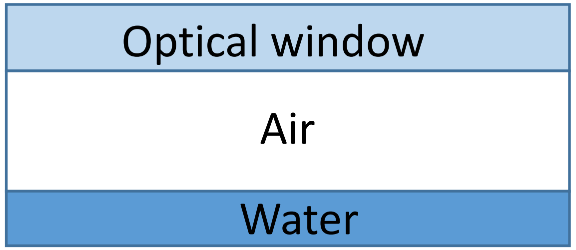

$t_{ag}(\lambda)$

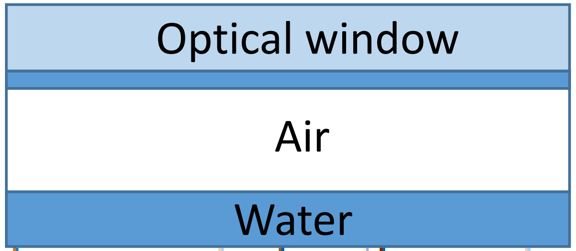

$t_{wa}(\lambda) \cdot t_{wg}(\lambda)$

Finally, $C_{ww}(\lambda) = t_{wa}(\lambda) \cdot t_{wg}(\lambda)/t_{ag}(\lambda)$ accounts for the wet optical window (idealized as a homogenous water film on the optical window) determined by the ratio of the combined transmittances of air-water and water-window interfaces $t_{wa}(\lambda) \cdot t_{wg}(\lambda)$ to that of an air-window interface $t_{ag}(\lambda)$, all computed applying the small angle approximation.

For completeness, it is mentioned that the corrections for the wet optical window C_{ww} exhibit values of approximately 1.3% slightly varying with λ in the 400-700 nm spectral interval. Laboratory verifications of such a correction showed values varying from a fraction of a percent to several percent depending on the size and spatial distribution of water drops on the optical window. Because of this, C_{ww} must be considered an idealized correction, still representative of the impact of water on the optical window of the SBA sensor.

Supporting the equivalence of the two methods

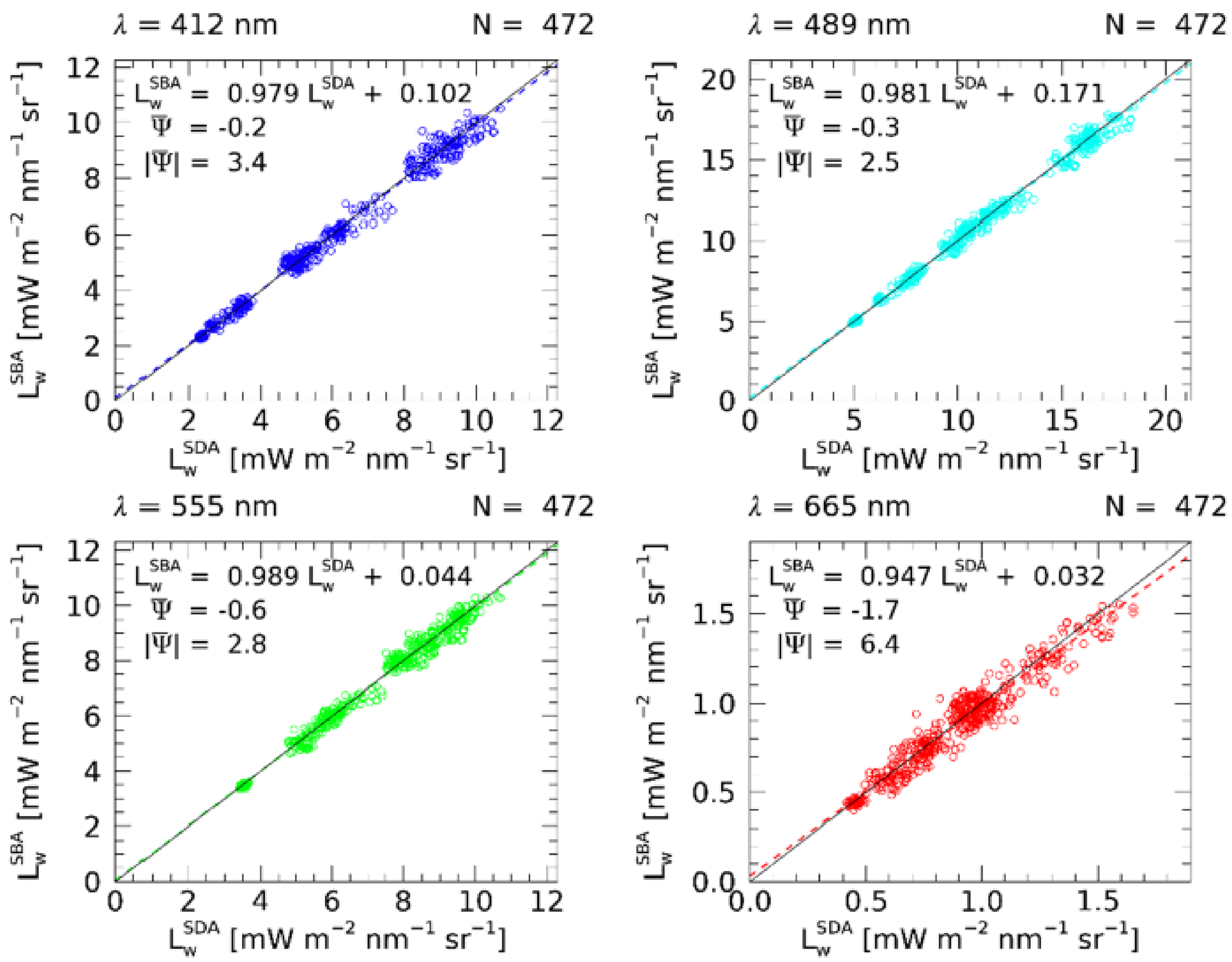

On the equivalence of the two methods

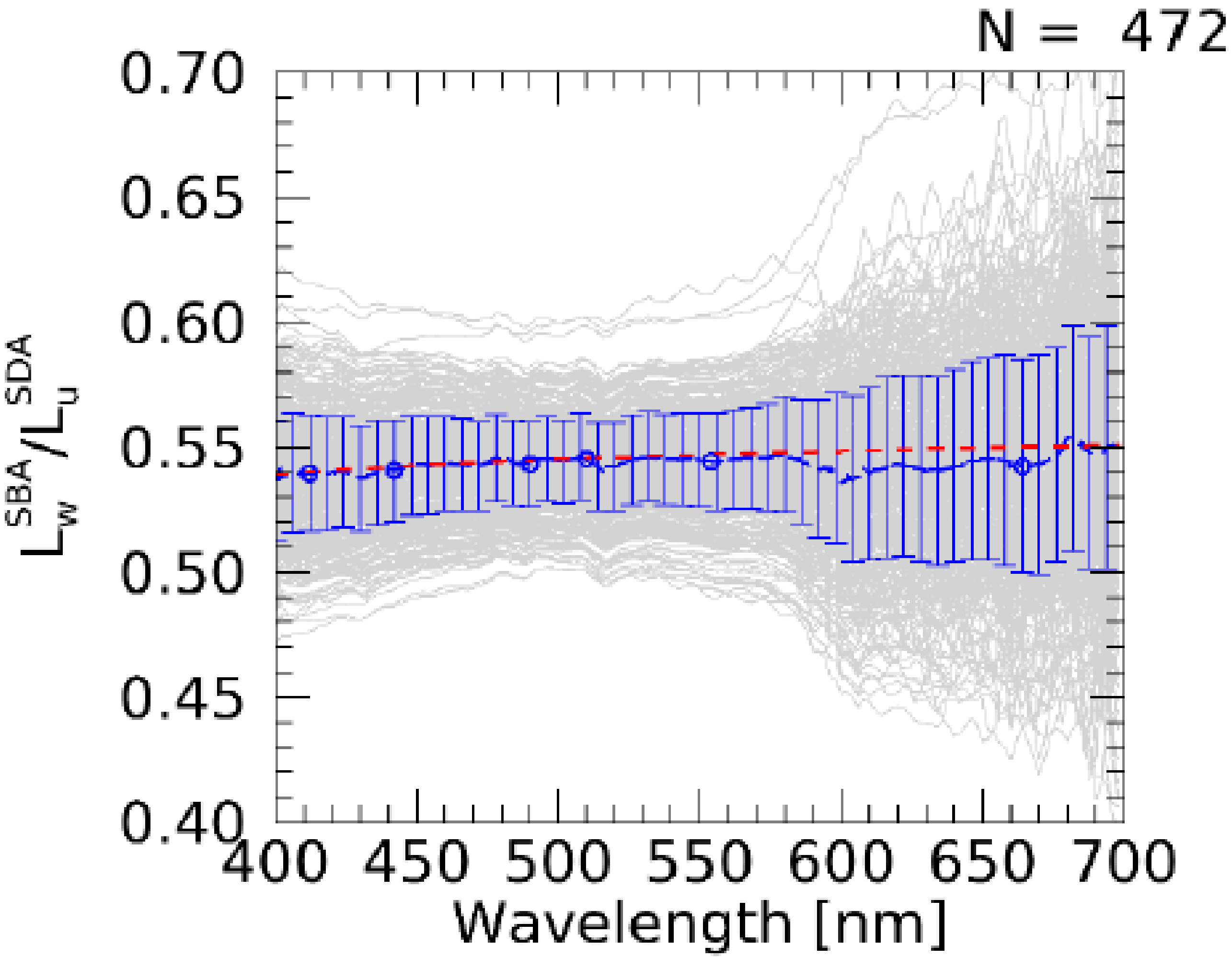

$$1/\frac{t_{wa}(\lambda)}{n_w^{\ 2}(\lambda)} = 0.54$$

On the equivalence of the two methods

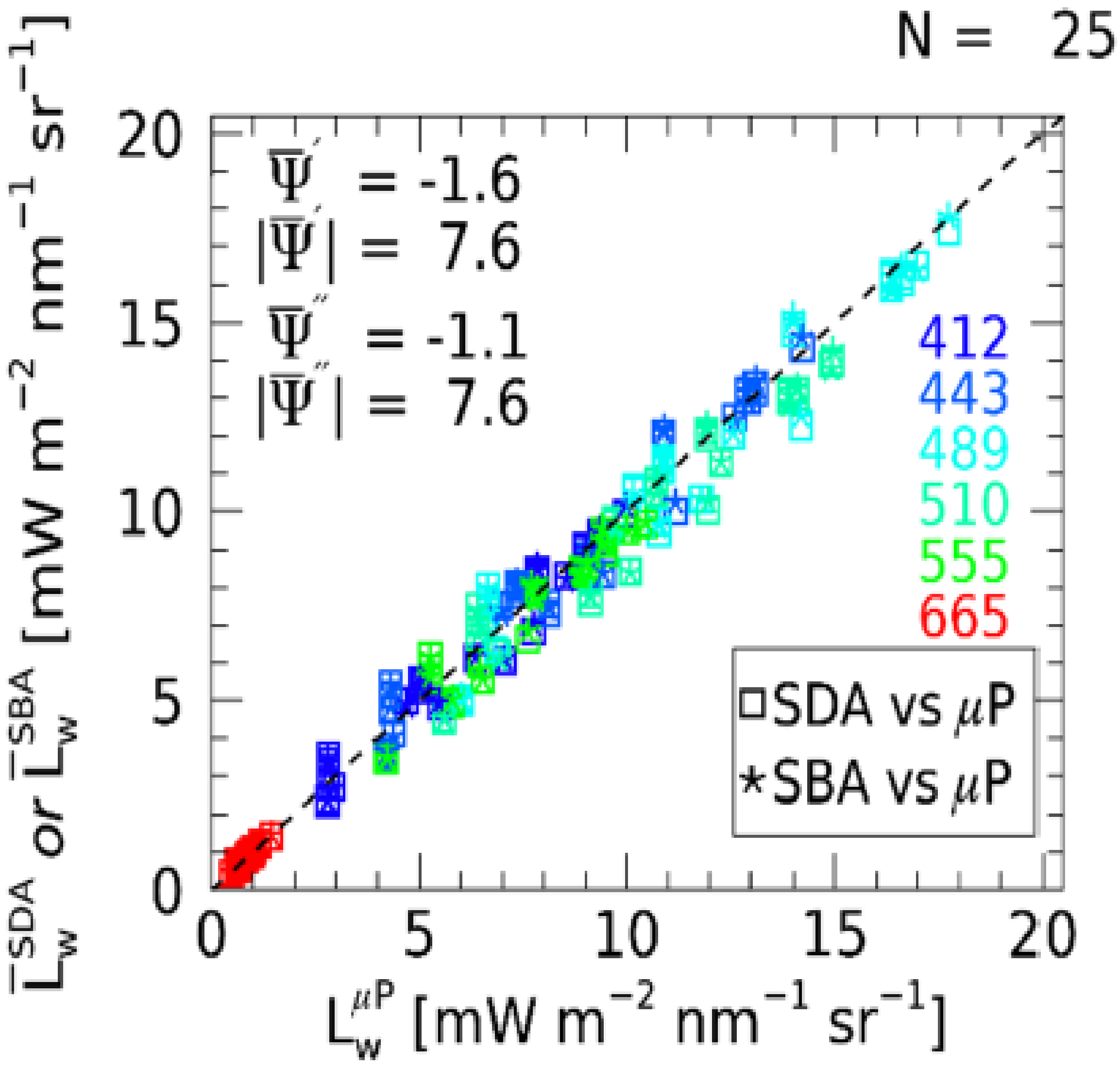

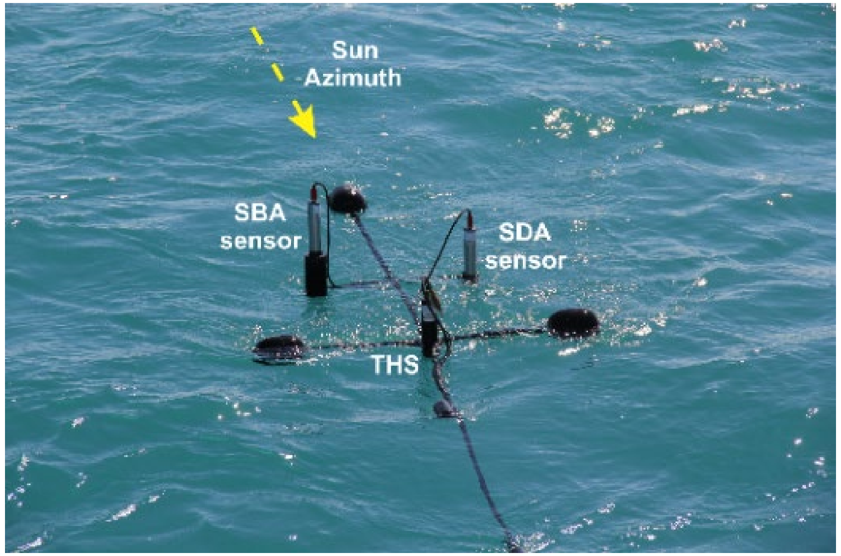

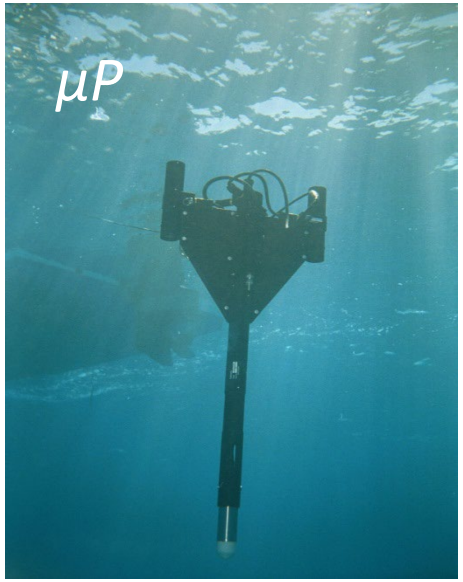

Conclusions

Near surface radiometric methods exhibit equivalence, which is fully supported by their inter-comparison and also their comparison with in-water radiometry methods.

Definitively, all radiometric measurement methods exhibit advantages and disadvantages.

Near-surface methods, comprehensively implemented, can easily support manned radiometric methods.

Still, above-water radiometry, benefitting of consolidated technology, accurate calibration and characterizations, comprehensive measurement protocols (implying the application of community-shared quality assurance, processing and quality control procedures) exhibit relevance for both manned and automated operations and has already amply shown the capability to support satellite ocean color applications.